

## Reverse osmosis powered by concentrating solar power (CSP): A case study for Trapani, Sicily

Sérgio Casimiro<sup>a,c,1,\*</sup>, Mahran K.A. Ahmed<sup>b</sup>, João P. Cardoso<sup>a</sup>, J. Farinha Mendes<sup>a</sup>

<sup>a</sup>Laboratório Nacional de Energia e Geologia, I.P., Lisboa, Portugal, email: sergio.casimiro@lneg.pt

<sup>b</sup>Loughborough University, Leicestershire, UK

<sup>c</sup>Sustainable Energy Systems, MIT-Portugal Program, Lisboa, Portugal

Received 1 August 2015; Accepted 15 July 2016

---

### ABSTRACT

The objective of this paper is to analyze the physical performance of two technologies in a water and electricity co-generation scheme: concentrated solar power (CSP) plant coupled to a reverse osmosis (RO) unit for a location in the city of Trapani, in southern Italy. The CSP+RO system is also compared with a multi-effect desalination (MED) unit powered by a CSP plant in the same location in Italy, adapting a model developed in a previous study [2]. The location of Trapani is used as it allows the comparison of the simulation results with an existing stand-alone gas powered commercial MED plant located at Trapani [3] (which has operated until very recently). This work was conducted using as the main simulation tools: the system advisor model (SAM) developed by the US National Renewable Energy Laboratory (NREL); a recent upgrade to SAM made available to this work through the Portuguese Laboratório Nacional de Energia e Geologia I.P. (LNEG); and the reverse osmosis system analysis (ROSA) developed by the Dow Chemical Company. A technical visit to a real commercial RO plant in the south of Portugal (Alvor) was conducted, and the data gathered was used in the validation of the ROSA model. The results for the Trapani case study show that the CSP-RO arrangement has the capability to produce ~46% of the total production of the full scale plant at Trapani, if operated at nominal capacity, year round. Also, the CSP-RO system provides ~14% more water and ~20% more electricity than the CSP-MED system throughout the studied period of one year. The two co-generation schemes provide promising potential to fight the issues related to fresh water shortages and dependency on fossil fueled desalination. Thus, they can aid in decreasing the effects associated with CO<sub>2</sub> emissions and climate change.

*Keywords:* Reverse osmosis; Concentrated solar power; System analysis; Multi-effect desalination; Solar; Desalination; Co-generation, System advisor model; Renewable

---

### 1. Introduction

The use of seawater desalination to provide fresh drinking water is a well-established and flourishing industry. The two main technologies used are thermal desalination and reverse osmosis (RO) membrane filtration. In the main market for the desalination industry—the Middle East—large scale desalination plants are heavily used for the production of fresh water. It is expected that at current

growth rates and global climate changes, water demand in the Middle East and North Africa (MENA) region alone is going to increase by around 50% in the next 35 years [1]. The utilization of renewable energy sources for the production of drinking water is of great global interest, as it can potentially provide a sustainable solution for fresh water production in regions like the Middle East. The work described in this paper falls under this framework. It focuses on studying the potential of seawater desalination systems powered by concentrated solar power (CSP)

\*Corresponding author.

<sup>1</sup>Present address: Center for Complex Engineering Systems, King Abdulaziz City for Science and Technology, Riyadh, Saudi Arabia.

Presented at EuroMed 2015: Desalination for Clean Water and Energy Palermo, Italy, 10–14 May 2015.

Organized by the European Desalination Society.

plants as a means of renewable desalination. RO and MED were selected to be analyzed in this work as they present the best performances within the mature technologies operating in the desalination market.

### 1.1. Methodology

The steps applied to perform this study are based on freely available computer modelling tools used for the simulation of RO and CSP operation. These steps include, firstly the validation of the reverse osmosis system analysis (ROSA) tool with operational data for nominal conditions from a small scale water desalination plant in Alvor, Portugal. Secondly, the utilization of the system advisor model (SAM) developed by the National Renewable Energy Laboratory (NREL) to simulate a CSP plant, together with ROSA to simulate the RO unit using data for the location of Trapani. The results of both models were combined to obtain the performance of a CSP-RO co-generation scheme. Thirdly, an analysis and comparison between: 1) the CSP-RO modelled; 2) a CSP-MED co-generation scheme previously studied in [2] adapted to the work shown in this paper; and 3) data from a real TVC-MED plant that exists in Trapani, Sicily [3].

## 2. Reverse osmosis system analysis (ROSA) tool

ROSA can be used to estimate the performance of a new RO system under design conditions, or the performance of an existing RO system under off-design conditions. This projected performance is based on the nominal performance specification for the DOW FILMTEC™ element(s) (or membranes) used in that system. Accurate results can be obtained very quickly using the ROSA computer program. Thus, it can be used to modify and optimize the design of an RO system. The entire system calculation methods will not be described in detail, however the major governing equations and parameters will be briefly described in this section. These equations were also used previous work [4] to develop a computer model, similar to ROSA, to predict the performance of RO systems based on membrane-to-membrane analysis (single element performance).

### 2.1. Design equations and parameters

The performance of a specified RO system, in ROSA, is defined by its feed pressure (or permeate flow, if the feed pressure is specified) and its salt passage (amount of salt passing through the membrane). In its simplest form, the permeate flow ( $Q$ ) through an RO membrane is a function of the membrane active area (wet area) ( $S$ ), the net driving pressure (NDP) ( $\Delta P - \Delta\pi$ ) and the membrane permeability. The permeate water flux can be calculated from the following equation [5]:

$$Q = (A)(S)(\Delta P - \Delta\pi) \quad (1)$$

Van't Hoff's theoretical osmotic pressure equation is adapted to operational conditions by DOW FILMTEC™, and then used to calculate the osmotic pressure of the feed solution:

$$\pi_f = 1.12 (273 + T) \sum m_j \quad (2)$$

For a given recovery rate, applied feed pressure ( $P_f$ ) increases with the increasing feed osmotic pressure. It should be noted that there's a minor drop in feed pressure as the feed solution passes from one membrane to another in the pressure vessel due to friction. Pressure drop in the concentrate side of an RO membrane can be estimated from the following equation:

$$P_{cd} = 0.01nq_{fc}^{1.7} \quad (3)$$

The average concentrate side flow rate ( $q_{fc}$ ), is equal to the arithmetic average of the feed and concentrate flow rates as in the following equation:

$$q_{fc} = \frac{Q_f + Q_c}{2} \quad (4)$$

In a typical RO process, as water flows through the membrane and the membrane rejects salts, a boundary layer is formed near the membrane surface in which salt concentration exceeds the salt concentration in the bulk solution by a factor equal to the concentration polarization value [5]. This parameter can be calculated from the following equation:

$$CP = \frac{C_{sp}}{C_b} \quad (5)$$

Experimentally, DOW FILMTEC™ has determined that  $CP = \text{EXP}(0.7R)$  where  $R$  is the recovery rate. Eq. (5) shows that the nominal salt rejection rate in RO membranes is lower than the true rejection rate. The actual rejection rate can be defined as the ratio between the permeate concentration to the feed concentration at the membrane surface:

$$R_j = 1 - (C_p/C_f) \quad (6)$$

Although the membranes are designed for high rejection, some amounts of salt always pass through the membranes. In the ROSA design equations, the salt passage is by salt diffusion through the membrane. Thus, the salt flux is proportional to the salt concentration difference between both sides of the membrane. The proportionality constant is known as the salt diffusion coefficient or the B factor.

$$NA = B (C_f - C_p) \quad (7)$$

The quality of the permeate is proportional to the B factor, concentration polarization, salt rejection, feed concentration and membrane active area. It can be calculate using the following equation:

$$C_p = B * C_{fc} * CP * R_j * \frac{S}{Q_p} \quad (8)$$

The permeate concentration  $C_p$  represents the quality of the treated water which is a function of membrane type and operational conditions such as feed water temperatures and total dissolved solids (TDS) levels. The permeate osmotic pressure can be calculated using the feed osmotic pressure as a reference:

$$\pi_p = \pi_f (1 - R_p) \quad (9)$$

Permeate flow through the RO membrane can be expressed more completely by rearranging Eq. (1) taking into account the effect of the permeate osmotic pressure, average pressure drop in the RO vessel, permeate pressure, and fouling factor Eq. (1) can be rewritten as follows:

$$Q_p = (A)(S)(TCF)(FF) \left( P_f - \frac{P_{cd}}{2} - P_p - \pi_{ave} + \pi_p \right) \quad (10)$$

The fouling factor is applied to simulate aging and loss of membrane permeability due to compaction and scale fouling. Typically a fouling factor of 1 is applied to new membrane, and a fouling factor between 0.65–0.85 for three year old membranes and onwards. Also, because the performance of the RO membranes is typically tested at 25°C, a temperature correction factor (TCF) is considered were suitable in the equations above to adjust the temperature differences when running simulations assuming other feed-water temperatures. TCF is determined using the following equations [5]:

$$TCF = EXP \left[ 2640 \left( \frac{1}{298} - \frac{1}{273+T} \right) \right]; T \geq 25^\circ C \quad (11)$$

$$TCF = EXP \left[ 3020 \left( \frac{1}{298} - \frac{1}{273+T} \right) \right]; T \leq 25^\circ C \quad (12)$$

### 3. ROSA validation

The reverse osmosis plant data used in the validation procedure were provided by the plant operators of a desalination plant in the southern city of Alvor, Algarve, Portugal on October 10<sup>th</sup> 2014. The plant has a water production of around 800 m<sup>3</sup> d<sup>-1</sup>, and the data referred to nominal operation of the plant.

#### 3.1. Plant configurations

The plant is composed of a pre-treatment system, 54 semipermeable membranes (9 pressure vessels with 6 membranes each) as seen in Fig. 1, an energy recovery system (based on pressure exchange from the brine directly



Fig. 1. Alvor plant membrane assembly.



Fig. 2. Energy recovery device.

to the feed, Fig. 2), and three main pumps: a low pressure pump (1 bar) between the intake and pre-treatment filters, a high pressure pump (60 bar) forcing the water through the membranes, and the energy recovering pump (56 bar). It also has a post-treatment system and a reservoir for produced water of 1000 m<sup>3</sup>. A high efficiency energy recovery system is used, it recovers energy by transferring most of the remaining pressure contained in concentrate stream to a portion of the total feed water mass flow. This system allows the mixing of a small amount of brine water (5–10%) with the supply water, which can compensate for minimum required salinity to run the membranes to produce the targeted permeate quality.

As part of this study, the reverse osmosis system analysis (ROSA) model, a product of DOW FILMTEC™, is validated against another manufacturer's desalination membranes (Toray). The objective was threefold: 1) learn about the design and operation of a RO plant and related software using real plant data as reference, 2) describe in the literature one of the few seawater RO plants operating in Portugal, 3) confirm that ROSA can be used to simulate the operation of a plant using membranes from other manufacturers with seawater instead of brackish water (similar research can be found in the literature [6], but it compares the performance of these software with real RO plant data making use of brackish water).

The Alvor plant uses Toray TM820C-400 membranes. These are high rejection seawater membranes, with an area of 37 m<sup>2</sup> per element that according to the manufacturer maximize productivity and enable predictive system design. The current membranes being used at Alvor were replaced in a successive manner, one by one, starting from the first maintenance operation carried out, and by May

2014, they had all been replaced. (the first element of each pressure vessel is normally replaced during each major maintenance operation, being the new replacement placed at the back of each pressure vessel).

In the validation procedure carried out in this work, it is assumed that all membranes are new. The RO cross reference tool [7] is used to determine the corresponding Dow membrane type with similar physical and operating characteristics to the ones used at the Alvor plant.

The plant is located at 17 m above sea level. It has three wells. One used as a water intake at –8 m below the sea level, one used to monitor the water level, salinity and temperature. In addition to a third well which acts as a brine discharge located at 30 m depth and connected to underground currents that carry the brine into the sea. It is the furthest away from the plant to ensure that no mixing occurs between the feedwater and the brine. The wells are located near the coast and the changing tide levels can have an impact on the operation of the plant by causing a mixture of underground fresh water streams with the seawater underground intake, which can lead to a decrease in the salinity of the feed water throughout the year (depending on the rainfall precipitation levels).

### 3.2. Validation input data

The validation of the ROSA model is done using the quality, mass flow rate, and temperature of the total feed water. The main parameters used in the validation are shown in Table 1.

### 3.3. Output results

The main results of the validation process are shown in Table 2, where real operational data at nominal conditions from the RO plant in Alvor are compared to the model outputs for the general operating parameters of permeate and concentrate flow rates and salinities, as well the feed pump pressure.

The model predictions fall in the line with the operational data from the plant, with an error margin of ~10%

Table 1  
ROSA validation inputs

Parameter	Value
Pre-stage $\Delta P$ , bar	0.345
Feed water salinity (TDS), mg l <sup>-1</sup>	33800
No. of passes	1
No. of stages	1
Flow factor	1
Recovery rate, %	40
Feed flow rate, m <sup>3</sup> h <sup>-1</sup>	87
Membrane type	SW30XHR-400i
No. of membranes in pressure vessel	6
No. of pressure vessels	9
pH	5.7
Water temperature, °C	18
Pump efficiency, %	80

Table 2  
ROSA validation outputs

Parameter	Real data	Modelled data	Difference (%)
Permeate flow rate, m <sup>3</sup> h <sup>-1</sup>	34.0	34.8	+2.4
Concentrate flow rate, m <sup>3</sup> h <sup>-1</sup>	54.0	52.5	-2.7
Permeate salinity, mg l <sup>-1</sup>	165	149.6	-9.3
Concentrate salinity, mg l <sup>-1</sup>	52988	55431	+4.6
Feed pump pressure, bar	60.0	55.5	-7.5

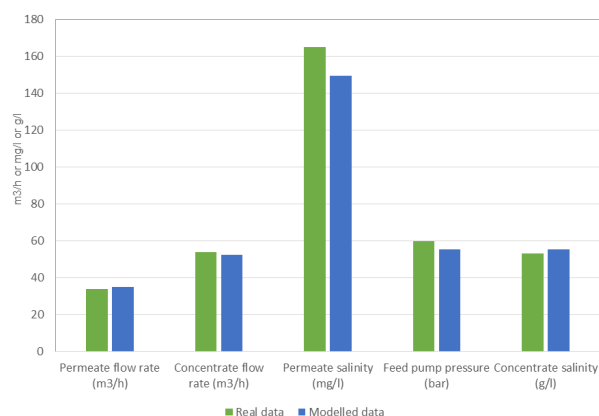


Fig. 3. RO real data vs. modelled data.

compared to the real plant outputs (Fig. 3). The most important finding is that the model under predicted the feed pump pressure by around 7.5%. These marginal differences can be attributed to simplifying assumptions within the models mathematical algorithms, and to the quality of the real data gathered. Performance parameters for nominal operation, regarding the water quality, were not collected during the technical visit to the plant, as it was not in operation during the site visit and a shutdown procedure in which fresh water is flushed through the membranes had been performed.

As some of the water used for flushing was mixed with each of the permeate and concentrate in the tanks, a direct measurements of conductivity would not return representative results of normal plant operation. The conductivity data provided by the plant operators were used to estimate the feed water total dissolved solids based on a derived conductivity-to-total dissolved solids conversion factor [6]. Although it eliminates time consuming analytical testing of the water, it is not the most accurate method for determining feed water TDS values.

Additionally, it is possible that ROSA incorporates a “safety factor” when predicting the required feed pressure, as it is used to size the feed pump(s). Such an embedded factor might influence the accuracy of the model, but gives a conservative approach from a design

perspective. A conservative prediction might increase the reliability of water production, but at the expense of less efficient operation. Overall, the authors conclude that the ROSA model provides an approximate estimate of system performance that can be used in early stages of RO system design.

#### 4. Case study

##### 4.1. System description

The main goal of this study is to simulate the performance of a parabolic trough plant coupled with a seawater desalination RO unit and compare it with an existing large-scale (thermal vapor compression) TVC-MED parallel feed desalination plant, capable of producing 36 000 m<sup>3</sup> d<sup>-1</sup> [8]. This MED plant was chosen as reference for this case study, firstly, because it is one of the few plants with detailed design information available in the literature. Secondly, because it was possible to use data from a previous study regarding the operation of this MED plant using natural gas versus the option of using a CSP plant as power source [2]. Thirdly, no relevant detailed comparison is available in the literature regarding the operation of CSP-RO, versus CSP-MED, versus the operation of an existing plant for the same site.

Such a coupling (CSP-RO) will initially assume that all the net electrical power output from the power block will drive the RO unit's high-pressure pump, pre and post-treatment, intake and outfall systems. The unit's main operating parameters, that is, the recovery and feed pressure, are established by considering membrane control and operation limits. The CSP-RO system modelled consists of a 49.4 MWe (gross production) parabolic trough CSP plant with a conventional steam Rankine cycle coupled with a large-scale two-stage RO plant (first stage assumed to have 49 pressure vessels, and second stage 36 pressure vessels, each pressure vessel with 6 elements). The RO system is divided into six parallel connected trains, to enable flexible partial operation (each train with 2 stages). The RO system has a total recovery of 45%, and energy is recovered using a high efficiency pressure exchanger. The first stage recovers 37.6%, and the second stage 11.8% (the second stage receives as feed the brine produced on the first stage). Each simulated RO train produces 6 000 m<sup>3</sup> d<sup>-1</sup> of fresh water, with a total of 36,000 m<sup>3</sup> d<sup>-1</sup> at nominal capacity (matching the output of the full-scale MED plant described in [2]).

The CSP+MED system shown here is adapted from the work presented in [2]. Since the release of the study performed in [2], the MED add-on to SAM has suffered continuous upgrades. The simulations for the CSP+MED system shown in this paper use an upgraded version of this add-on to SAM, that now makes use of new performance curves to simulate the Rankine cycle. This new upgrade allows the description of its operation with dedicated intermediate steam extractions to power the MED system (entering either a thermal vapor compressor, TVC, and/or the ejection system of non-condensable gases), though it will not be described in detail in this article, as it will be part of a future publication.

In the original study [2], the CSP+MED system was simulated assuming that the MED system is undersized

regarding the reference value of 100% for the nominal heat load output from the CSP plant (this is a user defined input), with the aim of improving the MED plant performance during part load operation of the CSP plant. This plant configuration favored the number of hours that the MED would operate at nominal capacity instead of optimizing the average cutback that the MED plant would impose on the electric production of the CSP plant. With that design, when the CSP exhaust steam heat load goes above the maximum heat absorption capacity of the MED plant (which in the simulation from [2] was set to 40% of the nominal heat load output from the CSP), the remaining exhaust steam is routed into the Sea Water Cooling Circuit (SWCC). The SWCC is set to operate at the same vapor pressure than the steam entering the MED plant. In these conditions, only part of the exhaust steam is being used to power the MED and produce fresh water. This produces an excessive cutback on electric production due to the forced condensation at high pressure of the entire mass steam flow, and not only of the steam flowing into the MED. On the other hand this strategy ensures that the MED plant will operate more times during the year at nominal capacity. Because of these it was decided to change the CSP+MED system configuration and assume that the MED plant would be sized for this study according to 100% of the heat load rejected by the CSP plant (1:1 ratio between CSP and MED). With this configuration a down condenser is considered only for the periods when the CSP plant operates below the minimum load required by the MED, and for shutdown and startup procedures.

To accommodate these changes to the CSP+MED configuration, the size of the CSP plant was reset to 49.4 MWe gross production and 44 MWe net, in the simulations shown in this paper—the minimum required to allow the operation of a 36 000 m<sup>3</sup> d<sup>-1</sup> MED plant in co-generation with a 1:1 ratio. At design the CSP rejected heat load equals the MED required heat load (if the CSP installed capacity would not have been reduced, the MED plant would need to be considered larger than 36,000 m<sup>3</sup> d<sup>-1</sup>, as it acts as the sole condenser of the power cycle with the new system configuration using the 1:1 ratio). The size selected for the CSP plant is much larger than necessary for the RO system (~49.4 MWe instead of ~6.7 MWe gross).

This study focuses especially on the water production of the CSP-RO system using four different cooling systems with the CSP plant: Wet cooling (using fresh water), wet cooling (using seawater), dry cooling and once-through seawater cooling assuming no grid connection in all cases. The location chosen for the system is the city of Trapani, in the southern island of Sicily, in Italy. The simulation for the CSP plant was done with the System Advisor Model's (SAM) (version 2014.1.14) physical trough model [9], using the integrated TRNSYS software program. SAM is a validated simulation program that can simulate the performance of CSP systems among other renewable energy systems using hourly resource data. The simulations for the CSP+MED, the once through and the seawater wet cooling systems are performed using the add-on recently developed for SAM [2]. Since the publication of the work described in [2] the upgrade performed to the add-on to SAM also includes a revised version of the once-through system, where now the user can set either that the SWCC during operation will maintain a stable vapor pressure in the condenser, or that it

will maintain a stable temperature difference between the saturated vapor pressure and the cooling water temperature outlet (this second option was used when simulating the CSP+ SWCC, operating with a variable vapor pressure to optimize the plant's performance).

It was defined that the CSP-RO system operates in a way that ensures that, in both full and partial operation of the CSP plant, each train is operated either at 100% capacity or it is shut down, depending on availability of power under different water temperatures across the simulation period (one year). Pumping costs of the seawater from the intake to the high pressure pump of the RO system are accounted for in this work. A minimum start-up and shutdown times are set for: the whole intake/outfall and pretreatment systems; and RO trains separately. The water temperatures are expected to range yearly within 10–22°C. A constant permeate flow in the RO trains is maintained by adjusting the feed pressure according to temperature in a way that keeps the same ratio of permeate flow against feed flow during operation. Fig. 4 shows a simplified scheme of the CSP-RO system considered in this work.

The source of water assumed for the evaporative cooling of the CSP plant is seawater when using an open sea surface water intake nearby the plant. The original SAM model has the option to simulate the operation of the CSP plant with wet cooling (using fresh water), dry cooling and hybrid cooling system (hybrid cooling is assumed to be mixture of wet and dry cooling, being the wet cooling turned ON when the price of energy or its demand is higher). Keeping in mind that this is an analysis at pre-design stage, most of the energy dissipation obtained with wet cooling comes from latent heat transfer instead of sensible heat, reducing significantly the amount of water usage. A few °C of difference in the cooling water have a smaller impact in the overall power consumption when using wet cooling vs. a once through cooling circuit. If a wet cooling system would be installed, then probably the intake of water would be

near the plant without extensive maritime works to build an intake for the collection of cooler water into the plant. It is important to note that the computer code developed for the once through cooling system was initially made for the assessment of CSP+MED. When using this configuration the condenser is "cooled down" with sensible heat transfer from the cooling water, and so using cooling water with a few °C lower has a bigger impact on the plant performance. Because of the reasons mentioned above, in this work it was considered that it would be neglected the power consumption to pump cooling water from the sea up to the wet cooling system, while the calculations when using a once through cooling circuit would account for that.

It should be noted that both the CSP and the MED models do not account for differences in the performance of similar power blocks or MED trains, when the only difference is the installed capacity.

It is being assumed co-location of the CSP and RO plants. Though, the intake for the RO is considered to be an open surface, while the CSP with a SWCC is considered to use a different underwater intake pipe stretching ~2800 m from the limit of the CSP plant (similarly to the intake system used by the real MED plant at Trapani).

#### 4.2. Simulation parameters

The design and simulation of the RO plant is aimed to meet a water production of 36,000 m<sup>3</sup> d<sup>-1</sup> matching the amount of water produced by a real MED plant in Trapani [8]. The CSP simulations used the predefined configuration found in SAM's physical trough model. The main changes were applied to the installed power, thermal storage hourly availability, solar multiple, and the weather data used to match the power capacity of the CSP-MED system in [2]. The weather file that was used was built by combining two sources: Meteonorm 5.1 database available in TRNSYS 16, and satellite data from the year of 1997 (from the latter namely, the global horizontal irradiance (GHI), the diffuse horizontal irradiance (DHI), both of these used to calculate then the DNI in TRNSYS). The original file from Meteonorm did not match the weather profile expected for the region, as it provided lower DNI values than expected from several other sources (~1310 kWh m<sup>-2</sup> y<sup>-1</sup> vs. >1800 kWh m<sup>-2</sup> y<sup>-1</sup>) [10,11]. The primary simulation inputs are displayed in Table 3.

The RO simulations are carried out using the ROSA model discussed in points 2 and 3. Several simulations were carried out to determine the optimum configuration for the RO plant, having into consideration the system design recommendations [5,12]. The selected RO system considered a total of 3060 membranes (considering all the RO trains and stages), each of them designed for high salt rejection and low energy consumption with an area of 40.9 m<sup>2</sup> each. ROSA was used to simulate one train only, and all 6 trains are considered identical in this system, thus, the whole RO system's performance can be estimated by multiplying the outputs from ROSA by the number of operating trains. The algorithm used considered that whenever the CSP plant produces electricity, the preset water temperature is read (water temperature affects the viscosity and subsequently the quality and flow rate of water through the membrane, therefore affecting RO system power consumption). Afterwards the algorithm checks whether the available power from the CSP system

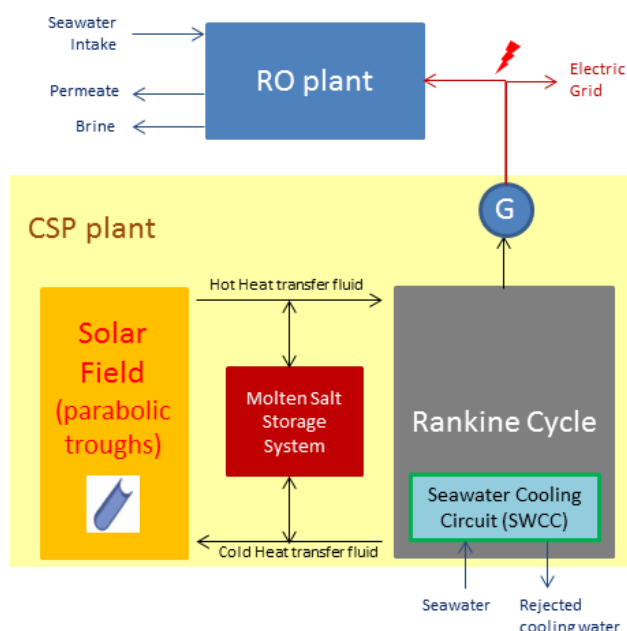


Fig. 4. Generic schematic diagram of CSP-RO system.

Table 3  
Main simulations inputs for SAM and ROSA

Input value	Value
<b>CSP Plant</b>	
Installed CSP power (PT using oil as HTF), MW <sub>e</sub>	44 net (49.4 gross)
Thermal storage, h	13
Rated cycle conversion efficiency, %	37.74
Condenser temperature for rated cycle conversion efficiency <sup>§</sup> , °C	35
Solar multiple*	3
Irradiation at design (reaching the solar field), W m <sup>-2</sup>	950
Total collector loop conversion efficiency (Solargenix SGX-1), %	71.69
Design inlet temperature, °C	391
Design outlet temperature, °C	291
Operating boiler pressure, bar	100
Hot standby period, h	2
Thermal power fraction for standby, %	20
Max. turbine overdesign operation, %	105
Min. turbine operation, %	25
Direct normal irradiation (DNI), kWh m <sup>-2</sup> y <sup>-1</sup>	2004
Fossil fill fraction <sup>†</sup> , %	0
<b>RO</b>	
Number of trains	6
Number of stages and passes / train	2 stages (each stage with only 1 pass)
Total number of pressure vessels / RO train	n = 85
Pressure vessels staging Ratio / RO train	49:36
Total number of membranes (entire RO plant)	n = 3 060
Feed water flow rate (entire RO plant), m <sup>3</sup> d <sup>-1</sup>	13 333
System recovery rate, %	45
Flow factor	1
Feedwater temperatures, °C	10(min)/22(max)
Feedwater salinity (TDS), mg l <sup>-1</sup>	40,000
pH	7.6
Pre-stage ΔP, bar	0.345
Membrane type	SW30HRLE-400i
Pump efficiency, %	90
Energy recovery device efficiency, %	90
Individual RO train start-up time, min	20
RO plant start-up time, min	130
Individual RO train shutdown time, min	15
RO plant shutdown time, min	130
% Energy consumption used with intake, pre-treatment and outfall vs. total RO plant consumption, %	30
<b>MED</b>	
Total number of effects (n)	12
MED designed fraction compared to CSP heat load output	1:1
Intake distance to MED plant, m	2 778
Saturated steam powering MED (this is the temperature defining the low pressure of the steam leaving the CSP turbine), °C	64.5
Seawater temperatures, °C	10(min) / 22(max)
Seawater salinity (TDS), mg l <sup>-1</sup>	40,000
Hot restart time <sup>‡</sup> , min	100

(Continued)

Table 3 (Continued)

Input value	Value
Overdesign (max. operation), %	100
Min. operation, %	20
Tv(1), °C	62.2
Tv(n), °C	37
Tf(n), °C	35
Motive steam pressure used with NCG ejection system, bar	8
Average heat loss per effect, %	0
Salinity of distillate produced (TDS), ppm	0
Once through seawater cooling	
Distance between plant and water intake tube, m	2000
Intake tube water velocity, m s <sup>-1</sup>	0.3
Temperature approach, °C	5
Distance between plant and end of brine discharge tube, m	2000
Brine tube water velocity, m s <sup>-1</sup>	0.3
Plant site elevation above sea level, m	10
Water storage tank distance from plant, m	100
Water storage tank height, m	5
Temperature approach between steam temperature and cooling water outlet, °C	5
Cooling water temperature rise across the condenser †, °C	10
Dry cooling	
Minimum condenser pressure, in Hg	2
Initial temperature difference at design, °C	16
Wet cooling	
Minimum condenser pressure, in Hg	1.25
Approach temperature, °C	5

\* The solar multiple makes it possible to represent the solar field aperture area as a multiple of the power block rated capacity. A solar multiple of one (SM = 1) represents the solar field aperture area that, when exposed to solar radiation equal to the design radiation value (irradiation at design), generates the quantity of thermal energy required to drive the power block at its rated capacity (design gross output), accounting for thermal and optical losses. [9].

† Fraction of the power block design turbine gross output from the power block that can be met by the backup boiler.

§ SAM sets the operation of the CSP plant by using amongst other inputs, the Rankine cycle's efficiency, and the condenser's saturated steam temperature at which the cycle operates with that efficiency.

‡ 100 min is a conservative estimate for a hot startup of an MED plant. An optimistic approach would be just above ~30 min.

¶ The calculation of the saturated temperature inside the condenser is done by summing: 1) the seawater temperature, with the temperature approach between steam temperature and cooling water outlet (user input); 2) the cooling water temperature rise across the condenser (user input); and 3) the a temperature difference at hot side of the condenser (preset at 3°C similarly to what is done to calculate the operation of the wet and dry cooling processes in the original SAM code).

is sufficient to run 6 trains and registers the corresponding water production. Otherwise, it runs the same test for 5 trains and so on in a descending manner until it reaches 1 train. If the power available is not enough to operate one train, the CSP-RO system does not produce any water and produces electricity only, and when the system produces water, the remaining power from the CSP is set as net electrical output. All the remaining electricity produced by the CSP that is not used by the RO system is considered to be available to be injected into the electrical grid or used by some other process that may be attached connected directly to the CSP plant. This controlling algorithm was implemented in Microsoft Excel environment, and its core is described in Fig. 5.

An ERD is an essential piece of equipment in modern RO plants to reduce the total power consumption, which is even more important when coupled with solar energy as its cost can still be higher than conventional power supplies. The operation of the RO plant in the simulations assumed an energy recovery device (ERD) though, ROSA does not allow the simulation of an RO system with ERD. To bypass this drawback, the RO system was simulated in ROSA without an ERD. After that the concentrate outlet pressure and mass flow rate from the first stage (for each of the considered operating feedwater temperatures through the year) was multiplied by the ERD efficiency (set at 90%). By doing this, it was possible to calculate power that could be

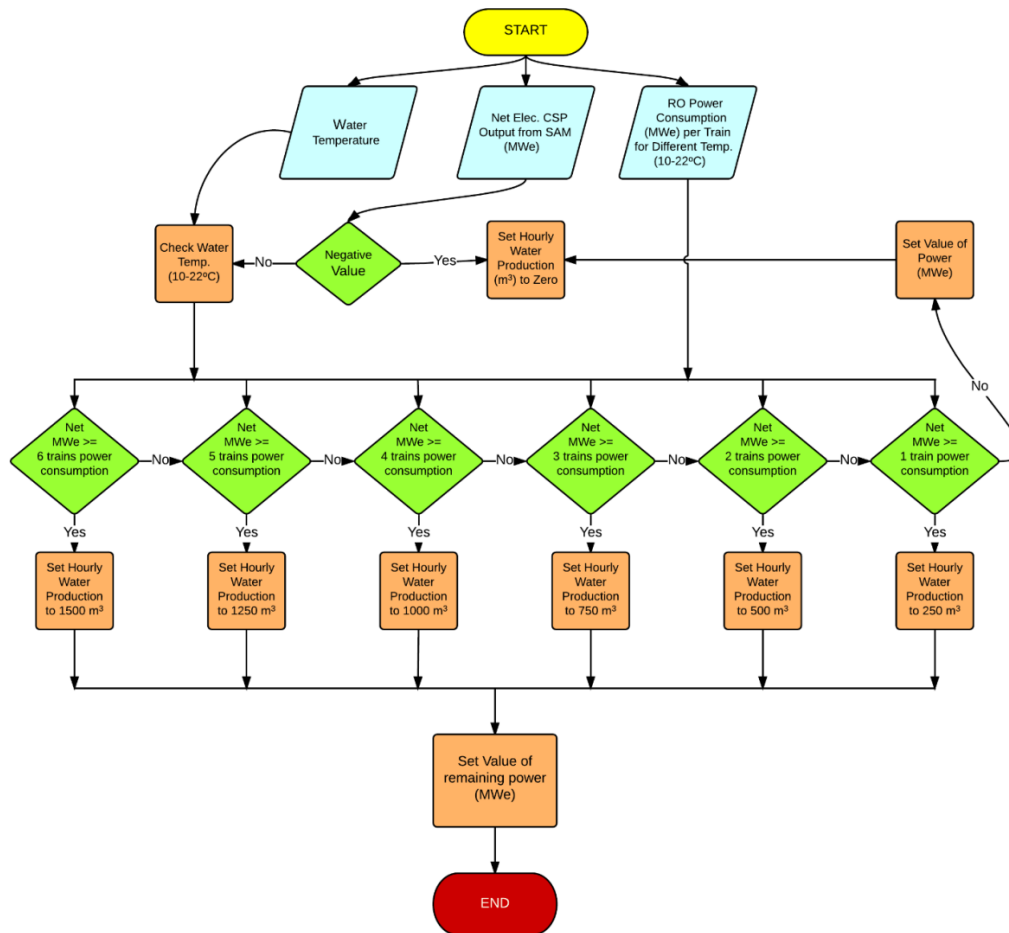


Fig. 5. Operational Strategy of CSP-RO System.

recovered by the ERD, and estimate the power consumption of each RO train using an ERD.

The start-up and shutdown time, and energy consumption of the RO plant intake and pretreatment system are also taken into account. After calculating how many RO trains can be operated at a given time (as described above), the controlling algorithm subtracts from the total permeate production (calculated for each hour) the amount of permeate corresponding to the time that the intake and pretreatment system was starting-up or shutting down (during this period the permeate produced by the RO trains is not assumed to be used). A ratio is used for the amount of power that the intake and pretreatment system use (30%) vs. the power consumption of the RO trains alone. Every time an RO train is started-up/shutdown while the intake and pretreatment system is already online, the corresponding RO train startup/shutdown time and energy consumption are also accounted with a negative impact on the total permeate production. During a startup of an RO train, it was assumed that it will produce only half of the permeate it could produce at full capacity during that period of time (the aim was to simulate a ramping up of the RO train production during startup). During shutdown of an RO train all the permeate produced is assumed to be wasted.

The CSP-RO system is configured so that at least between May and August the capacity factors are between 65–85%, and 70–80% for the CSP and RO plants respectively, aiming to reach the maximum number of hours of continuous operation by exploiting the increased availability of solar energy during that period.

#### 4.3. Results and discussion

Using the chosen designs and configurations for the simulations, the resulting yearly capacity factors for the CSP+RO system (considering the net electrical output) are between ~43–46% for the CSP and an average of ~46% for the RO system depending on the utilized cooling method. The financial factors were not used to optimize the size of CSP-RO system as economic costs are not accounted for in this study. Thus, it was not possible to determine the LCOE (levelized cost of energy) and the equivalent for water that would otherwise be used as a metric to size the CSP plant. The simulation results showed that the differences between yearly water productions under the four cooling system are minimal, in which all produce around 6,100,000 m<sup>3</sup> y<sup>-1</sup>. The two wet cooling options (seawater and freshwater), and the once-through system returned the highest net electricity

production ( $\sim 156,700 \text{ MWh}_e \text{ y}^{-1}$ ) and were almost inseparable in performance. Using saltwater might be costly in the long run as it can cause faster degradation of plant components [13] (when comparing a wet cooling system using freshwater vs. salt water). When comparing the cooling temperatures provided by the wet cooling system vs. the once-through, the once-through system provided lower temperatures during the warmer months, but warmer temperatures during the colder months. A shorter intake system to the plant could eventually ensure better performance of the once-through system, though it would be dependent on the temperature of the water it could obtain at shallower depths. Dry cooling is the worst in terms of power output, as it relies on the dry bulb temperature, which implies higher temperature in the down condenser of the Rankine cycle. It produces around 7% less than the wet cooling options. The summary with the total yearly production of fresh water and electricity (net) using the different technologies assumed in the simulations, are presented in Table 4 (results for wet cooling using fresh and seawater are shown as one entrance as their performance is very similar).

Although the CSP plant produces significantly more electricity during the summer, the RO system capacity remains the same and cannot consume the available extra energy, resulting in an increase of the net electrical production available for other uses during those months. Assessing the quality of water produced (permeate) throughout the year in Fig. 6 it is seen that the levels of TDS increase as water temperatures increase and vice versa. The variation in temperature affects the salt diffusion across the membranes and flow rates, and since the salinity of the feed water is fixed during the simulations and the amount of pressure applied depends on the quality of the water treated, the feed pump continues to apply pressure without considerable changes throughout the year, countering most of the changes in flow due to increase of temperature. Therefore, both feed pressure and flow rates through the system are considered constant throughout the year. Thus, the produced water quality is only affected by the changes in temperature. Today an increasing number of reverse osmosis systems use electrical motors with variable speed drives that can adjust both flow and feed pressure of the pump over a broad range, with little losses in efficiencies to enable further control of permeate quality. The average water quality for the simulation period of one year using the CSP-RO studied system, is  $\sim 156 \text{ mg l}^{-1}$  TDS, satisfying WHO (World Health Organization) standards, that allow a maximum

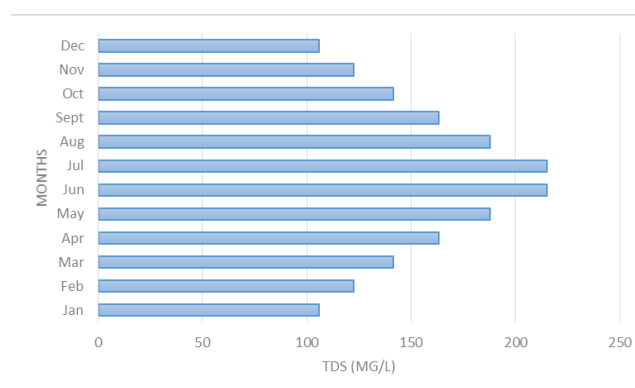


Fig. 6. Water quality across the year.

salinity of  $250 \text{ mg l}^{-1}$  for drinking water. The results of the CSP-RO simulations show that the choice of cooling system does not affect the water production by much, only the amount of electricity generated. Additionally, all performance parameters are within close margins of each other. The selection of the configuration using a cooling system depends mostly on site location and availability of water for cooling. The specific energy consumption of the RO system with the ERD system (excluding the energy consumption with the intake and pre-treatment system) ranged between  $\sim 2.80\text{--}2.5 \text{ kWh m}^{-3}$  (winter/summer). If accounting the intake and pretreatment system, these values would rise to a range between  $\sim 3.64\text{--}3.27 \text{ kWh m}^{-3}$ . The yearly average specific energy consumption (with ERD and intake and pre-treatment systems) was  $3.79 \text{ kWh m}^{-3}$ . This value is higher than the range mentioned previously due to multiple start-up and shut down of the intake, pretreatment and RO trains caused by the intermittent power supply from the solar plant during the year. During these events, energy is being consumed but no permeate being produced, penalizing the specific energy consumption of the RO plant.

The CSP+MED system considered for this work, presented a net capacity factor of  $\sim 34\%$  for the CSP plant ( $\sim 42.5\%$  gross), and  $\sim 40.5\%$  for the MED plant. It is important to note that the water quality output from the MED system (normally below 50 ppm) would be considerably better than from the RO system (with the configurations used).

#### 4.4. Comparison of technical performances

In this section, the performance of the CSP-RO system described above is compared to a CSP-MED system. This CSP+MED system, consists of a  $49.4 \text{ MW}_e$  (gross) parabolic trough CSP plant coupled with a low-temperature MED parallel-feed plant, using the add-on previously mentioned in 4.1. Both the CSP+RO and CSP+MED systems are assumed to be connected to once-through cooling system. With the configuration set in this work for the CSP+MED, the SWCC only operates during startup, shutdown, and part load operation of the CSP plant below the minimum load required by the MED. It is assumed that the most likely configuration for the CSP+RO will be installed near the sea, and therefore using seawater with a once through condenser. This configuration also allows a more straightforward comparison of results with the CSP+MED/SWCC configuration. On the CSP-MED simulation, the SWCC is

Table 4  
Total outputs summary for  $\text{m}^3$  of fresh water produced and net electrical production with the different configurations assumed

CSP+RO (Wet cooling)		CSP+RO (Dry cooling)	
$\text{m}^3 \text{ y}^{-1}$	$\text{MWh}_e \text{ y}^{-1}$	$\text{m}^3 \text{ y}^{-1}$	$\text{MWh}_e \text{ y}^{-1}$
6 091 563	156 748	6 091 125	144 895
CSP-RO/SWCC		CSP+MED/SWCC	
$\text{m}^3 \text{ y}^{-1}$	$\text{MWh}_e \text{ y}^{-1}$	$\text{m}^3 \text{ y}^{-1}$	$\text{MWh}_e \text{ y}^{-1}$
6 097 344	156 565	5 353 852	131 121

designed to absorb the total amount of rejected heat by the CSP plant at design conditions. The reason why this was done was because this would enable the operation of the CSP plant independently of the MED, which might be an advantage especially for the first systems to be built with CSP+MED, as mistakes with the startup and shut down of the MED plant may occur easily with the intermittency of the CSP plant. Also the simulation of the CSP+MED system assumed that during startup of the MED the dissipation of heat is done by the SWCC. This is a simplification, as in reality part of the steam leaving the CSP plant would be increasingly directed to the MED plant until it would reach the required level of operation. Also, the water produced by the MED plant during startup might not be of good quality, so it is not accounted when considering the total water produced by the MED.

Both the RO and MED systems being compared have a nominal production capacity of 36,000 m<sup>3</sup> d<sup>-1</sup> (the same as the real TVC-MED plant at Trapani). Analyzing the performance of the two, in Fig. 7, it is clear to see that the production profile is in line with the typical Mediterranean climate, peaking during summer and sharply declining during winter time, despite the use of a large thermal storage capacity, and a solar multiple of three for both CSP-MED and CSP-RO system. The rate of parasitic consumption also falls in line with this profile. The CSP parasitic consumptions accounted and described in [9] include auxiliary boiler parasitic load, fixed parasitic load, balance of plant parasitic load, total parasitic power for tank freeze protection, solar collector assemblies drives and electronics parasitic power, thermal energy storage and power block heat transfer fluid pumping power, collector field required pumping power, power block cooling parasitic power, and collector field required freeze protection parasitics and the pumping power for RO and MED in each system. Overall the CSP-RO/SWCC system has more parasitic consumption than the CSP-MED/SWCC as seen in Fig. 9. The reason is that the MED system does not use a high pressure pump. Therefore, the pumping power required for the RO is higher than for the MED. Despite that, the CSP-RO system produces more electricity throughout the year as coupling MED to a CSP plant introduces a higher cutback on the potential electric production of the power block of the plant due to the high thermal extraction of the MED when compared with the energy consumption of the RO plant (which is also a cutback in practice).

The CSP-RO system increases its performance compared to the CSP-MED through the warmer months of the year, regarding the net electricity (Fig. 7), and in the colder months regarding the water production (Fig. 8). The production of electricity and water is much lower during the winter months than in the summer time for both CSP-RO and CSP-MED systems, as the solar resource is scarce during this period for the studied location. Compared to the CSP-MED system, the CSP-RO system produces significantly more fresh water during the winter months, particularly in November and December in which the CSP-RO produces more than double of that of the CSP-MED. That is because of two main reasons. Firstly, there are several days during this period where the CSP-MED plant will not operate at all, or the CSP will operate at capacities below the minimum for the MED to work, while CSP-RO would still

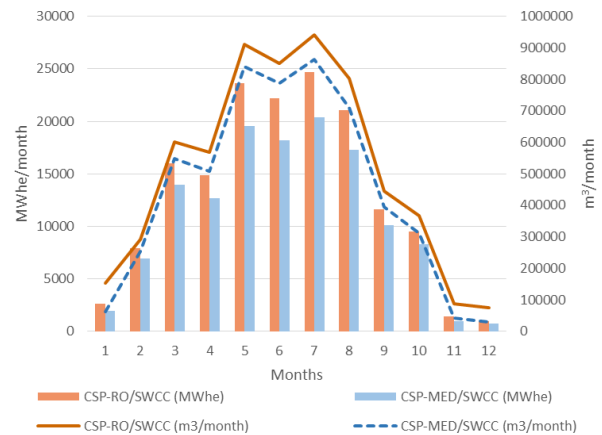


Fig. 7. Comparison of net electrical and water production.

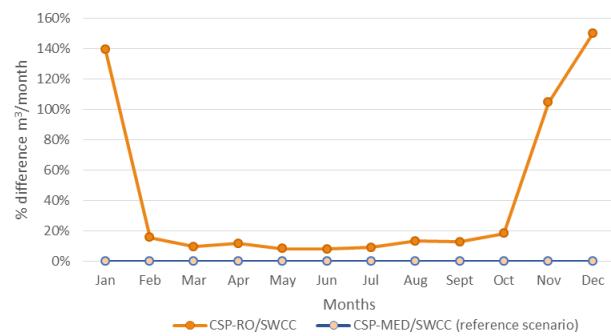


Fig. 8. Percentage of difference of water production.



Fig. 9. Comparison of parasitic consumption.

operate due to higher performance affiliated with the cooling system in comparison to the CSP-MED. Secondly, the MED system was configured as a large single train, while for the CSP-RO simulation the RO plant was subdivided into 6 trains (allowing a smoother part load operation).

Overall, the CSP-RO system (using a SWCC) provides around 20% more electricity and 14% more water throughout the year compared to CSP+MED. The calculated overall specific energy consumption is 3.79 kWh m<sup>-3</sup> for the CSP-RO system and 3.56 kWh m<sup>-3</sup> for the CSP-MED (water pumping only). Though, the MED coupling to the CSP plant introduces an overall cutback on the potential electric

production of the CSP plant equivalent to  $9.07 \text{ kWh m}^{-3}$  (considering the net power produced for the Trapani case study), while for the CSP+RO system this cutback is equal to the specific power consumption of the entire RO plant (the same  $3.79 \text{ kWh m}^{-3}$ ).

The performances of the two systems for a typical day in winter (January 3<sup>rd</sup>) and summer (July 1<sup>st</sup>) can be seen in Figs. 10 and 11. In the winter day, the lack of solar irradiation prevents nominal operation, and both plants are only able to operate for a few hours. The CSP-RO plant can only start to produce water at around 12 pm, and produces water at nominal capacity for a period of 6 h, during which the CSP-MED system starts producing water only an hour later, with nominal production occurring only for a short period. The CSP-RO system produces in total, more water than the CSP-MED. In the summer day, both systems operate at near nominal capacity production of  $1500 \text{ m}^3 \text{ h}^{-1}$  throughout the day, while the CSP-RO system produces slightly more electricity than the CSP-MED. The lower production of the CSP+MED system during the night is due to a slight cutback determined by the CSP plant controller originally built-in SAM. It is important to note that the previous discussion is valid only for the configurations discussed in this work and not generally valid for all kinds of CSP-MED integration schemes vs. CSP+RO, as they are very dependent on the detailed configurations of all these plants.

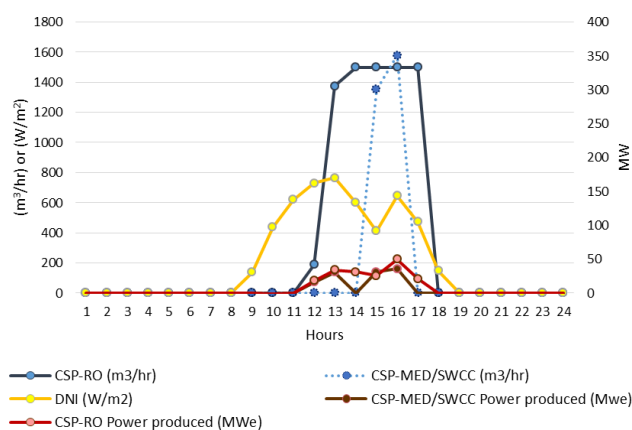


Fig. 10. Typical performance in a winter day.

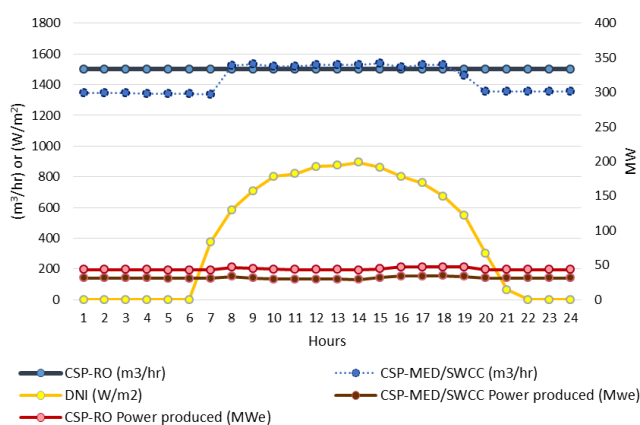


Fig. 11. Typical performance in a summer day.

Comparing the production of both systems (CSP+RO and CSP+MED) it is clear that to operate the desalination plants near nominal capacity similarly to the real commercial plant at Trapani, these co-generation systems would need to be significantly oversized to more than 2 times the installed capacity (as capacity factors of both desalination plants are between ~41 and ~46%).

## 5. Conclusions

This work presents the results for the yearly physical performance of a potential CSP-RO vs. CSP+MED systems operating in a co-generation scheme with no grid connection, for a location where a commercial large scale stand-alone MED plant has operated until very recently near the city of Trapani, west Sicily, Italy. This integrated comparison between RO and MED technologies powered by CSP is a novelty as far it was possible for the authors to verify in the literature regarding the level of detailed results presented for a case-study in specific location where it is also possible to compare with data from a real commercial plant.

This work was conducted using a commercial reverse osmosis computer model (ROSA) developed by DOW FILMTEC™ and a software developed by NREL capable of simulating the hourly operation of a CSP plant, with the aid of an add-on described in a previous work [2], and upgraded recently since then.

The CSP plant considered in the simulations had  $49.4 \text{ MW}_e$  ( $44 \text{ MW}_e$  net) at design, while both the MED and RO plants assumed a nominal water production of  $36,000 \text{ m}^3 \text{ d}^{-1}$ . Per year, the CSP+MED system has a net electric production of  $\sim 131 \text{ GWh}_e$  and  $\sim 5.3$  million  $\text{m}^3$ , and the CSP+RO has  $\sim 150 \text{ GWh}_e$  and  $\sim 6.1$  million  $\text{m}^3$ . The CSP-MED configuration has capacity factors of 33.7% and 40.6% for the CSP and MED plants, respectively, while the CSP-RO had capacity factors of 46.1% and 46.4% for the CSP and RO plant, respectively (using a SWCC as cooling system).

The results are in favor of the CSP-RO configuration (with SWCC or wet cooling) for the case study of Trapani, as the first produces around 20% more electricity and 14% more water throughout the year when compared to CSP+MED. Though it is important to have into account that the expected margin of error for the models used to simulate the plants is within  $\pm 10\%$  [9].

Results show that there are minimal differences in water production for the CSP-RO system using any of the four cooling options considered in this work (wet cooling with fresh and saltwater, dry cooling and a once through condenser). Regarding the electrical production of the CSP+RO, using wet cooling (with fresh or salt water) or a once-through seawater cooling (SWCC) system return very similar results, while using a dry cooling system would imply a cutback on electrical production of  $\sim 7\%$ . The electric production follows a typical seasonal pattern similar to that of most CSP systems in the Northern hemisphere, in which lower levels of production occur in the winter, and the highest level in summer, due to the increased availability of solar irradiation.

The CSP-RO provides significantly more electricity during the summer, while more than doubling the water production of the CSP-MED during some months in winter. The MED consumption for pumping only ( $3.56 \text{ kWh m}^{-3}$ )

is slightly lower than overall specific energy consumption of the RO plant (3.79 kWh m<sup>-3</sup>) which highly depends on the salinity of the input water. Though the overall cutback of electrical production of the MED plant corresponds to 9.07 kWh/m<sup>-3</sup>.

From the analysis above, the electricity yield of the CSP-MED is considerably lower when compared with CSP+RO. This is due to the high cold end temperature of the steam turbine which results in the delivery of less mechanical work to the power generator, when compared to a case using a steam turbine with a lower cold end temperature (as it happens with the CSP+RO). In order to produce the water amount equal to the full scale plant found at Trapani (that operates near design capacity during the year if necessary), the solar desalination systems simulated in this work would need to have more than double of the installed capacity.

During the execution of this work it was also possible to validate the ROSA model with data from an existing RO plant in Alvor, located in the Southern region of Portugal, Algarve. The results show that the main performance outputs such as, flow rates and salinities of the permeate and concentrate and the feed pump pressure fell within a 10% margin of error compared to the full-scale data used.

### Acknowledgements

The authors would also like to thank both Eng. David Loureiro and Cátia Jorge from LNEG for their help organizing and collecting data from the technical visit to the Alvor RO plant. Additionally, the author would like to extend the gratitude to the members of the Pestana Hotel Management. Eng. Joaquim Santos, Eng. Pedro Rosendo França and Mr. Paulo Justino for providing the opportunity to visit and collect data from the Alvor plant. The authors would also like to acknowledge the EU and the seventh framework program for the financial support of this work under the STAGE-STE project with contract number 609837.

### Symbols

S	—	Membrane area (m <sup>2</sup> )
A	—	Water permeability constant (l m <sup>-2</sup> h <sup>-1</sup> bar <sup>-1</sup> )
B	—	Salt permeability constant (m d <sup>-1</sup> )
C <sub>b</sub>	—	Bulk concentration (mg l <sup>-1</sup> )
C <sub>f</sub>	—	Feed concentration (mg l <sup>-1</sup> )
C <sub>fc</sub>	—	Concentrate feed concentration (mg l <sup>-1</sup> )
CP	—	Concentration polarization factor (-)
C <sub>p</sub>	—	Permeate concentration (mg l <sup>-1</sup> )
C <sub>w</sub>	—	Membrane surface concentration (mg l <sup>-1</sup> )
FF	—	Fouling factor (-)
Q	—	Permeate water flux (l m <sup>-2</sup> h <sup>-1</sup> )
n	—	Number of RO elements in series (-)
NA	—	Salt flux (-)
Σmj	—	Sum of molality concentration of all constituents in a solution (moles of solute/kg of solvent)
P <sub>cd</sub>	—	Concentrate side pressure drop (bar)
P <sub>f</sub>	—	Feed pressure (bar)

P	—	Permeate pressure (bar)
ΔP	—	Membrane pressure gradient (bar)
Q <sub>c</sub>	—	Concentrate flow rate (m <sup>3</sup> h <sup>-1</sup> )
Q <sub>f</sub>	—	Feed flow rate (m <sup>3</sup> h <sup>-1</sup> )
Q <sub>p</sub>	—	Permeate flow rate (m <sup>3</sup> h <sup>-1</sup> )
Q <sub>fc</sub>	—	Average concentrate side flow rate (m <sup>3</sup> h <sup>-1</sup> )
R	—	Recovery rate (-)
R <sub>j</sub>	—	Membrane rejection rate (-)
T	—	Feed temperature (°C)
TCF	—	Temperature correction factor (-)
Δπ	—	Osmotic pressure gradient (bar)
π <sub>ave</sub>	—	Average concentrate side osmotic pressure (bar)
π <sub>f</sub>	—	Feed osmotic pressure (bar)
π <sub>p</sub>	—	Permeate osmotic pressure (bar)

### References

- [1] MENA Development Report – “An Emerging Solution to Close the Water Gap in the Middle East and North Africa”, The World Bank, 2012.
- [2] S. Casimiro, J. Cardoso, C. Ioakimidis, J. Farinha Mendes, C. Mineo, A. Cipollina, MED parallel system powered by concentrating solar power (CSP). Model and case study: Trapani, Sicily, *Desal. Wat. Treat.*, 55(12) (2015) 3253–3266.
- [3] C. Temstet, G. Canton, J. Laborid, A. Durante, A large high-performance MED plant in Sicily, *Desalination* 105 (1996) 109–114.
- [4] A. Altaee, Computational model for estimating reverse osmosis system design and performance: Part-one binary feed solution, *Desalination*, 291 (2012) 101–105.
- [5] Dow Water & Process Solutions; FILMTEC™ Reverse Osmosis Membranes Technical Manual.
- [6] E. Mancha, D. DeMichele, W.S. Walker, T.F. Seacord, J. Sutherland, A. Cano, Part II. Performance Evaluation of Reverse Osmosis Membrane Computer Models”, Texas Water Development Board, 2014.
- [7] Dow Chemical Company, 2014, Reverse Osmosis Cross Reference Tool. Accessed: 23 September 2014, < <http://www.dow-waterandprocess.com/en/resources/ro-cross-reference-tool> >.
- [8] A. Cipollina, G. Micale, L. Rizzuti, A critical assessment of desalination operations in Sicily, *Desalination*, 182 (2005) 1–12.
- [9] M. Wagner, P. Gilman, Technical Manual for the SAM Physical Trough Model, Technical report NREL/TP- 55000-51825, National Renewable Energy Laboratory, Golden, CO, 2011.
- [10] GeoModelSolar, 2011, SolarGIS-Solar-map-DNI-Italy-en.png. Assessed 30 September 2014 <[http://solargis.info/doc/\\_pics/freemaps/1000px/dni/SolarGIS-Solar-map-DNI-Italy-en.png](http://solargis.info/doc/_pics/freemaps/1000px/dni/SolarGIS-Solar-map-DNI-Italy-en.png)>.
- [11] ABB, Technical Application Papers No. 10: Photovoltaic plants. Assessed 30 September 2014, <[http://www04.abb.com/global/seitp/seitp202.nsf/c71c66c1f02e6575c125711f004660e6/d54672ac6e97a439c12577ce003d8d84/\\$file/vol.10.pdf](http://www04.abb.com/global/seitp/seitp202.nsf/c71c66c1f02e6575c125711f004660e6/d54672ac6e97a439c12577ce003d8d84/$file/vol.10.pdf)>.
- [12] A.M. Delgado-Torres, L. Garcia-Rodriguez, V.J. Romero-Terreno, Preliminary design of a solar thermal-powered reverse osmosis system, *Desalination*, 216 (2007) 292–205.
- [13] J. Maulbetsch, M. DiFilippo, Performance, Cost, and Environmental Effects of Saltwater Cooling Towers, California Energy Commission, PIER Energy-related Environmental Research Program, Berkeley, CA, 2008.
- [14] G. Iaquaniello, A. Salladini, A. Mari, A.A. Mabrouk, H.E.S. Fath,, Concentrating solar power (CSP) system integrated with MED-RO hybrid desalination, *Desalination*, 336 (2014) 121–128.